Persistent properties of crises in a Duffing oscillator

Yao Huang Kao
Department of Telecommunication Engineering, National Chiao Tung University, Hsinchu, Taiwan 300 50, Republic of China

Jeun Chyuan Huang and Yih Shun Gou
Department of Electrophysics, National Chiao Tung University, Hsinchu, Taiwan 300 50, Republic of China
(Received 2 February 1987)

Crises in a two-well forced oscillator of Duffing type are studied with an analog simulation. Its features are discussed with the aid of return maps and phase portraits. Two types of boundary crisis in a strange attractor following the Feigenbaum route to chaos are found. One is associated with a hopping between two strange attractors and is confirmed with the presence of $1/f$ noise spectrum. The other is associated with a hysteresis jump. A borderline of differentiating these two characters is also indicated.

I. INTRODUCTION

Studies of chaotic motions in nonlinear dissipative systems are of great interest and have received much attention in recent years.[1,2] The chaotic motion may exhibit a crisis event with sudden qualitative change of a strange attractor as a controlled parameter is varied. According to Grebogi, Ott, and Yorke,[3] the crisis in a one-dimensional quadratic map occurs at certain parameter values, for which the strange attractor collides with an unstable periodic orbit. Since then, the crisis has been confirmed experimentally in several physical systems, including Josephson junctions[4,5] and some nonlinear driven oscillators.[6–8] In particular, the analog simulation of the rf-driven Josephson junction performed in our previous work[5] further indicates that the crisis induces either a hopping state with $1/f$ low-frequence noise or a hysteresis jump for different parameters set. Nevertheless, the occurrence of these two effects related to the crisis is not yet fully understood. In fact, we note that a global description of persistent properties of the crisis in diverse physical systems is still necessary to find in order to elucidate a true mechanism of the crises in chaotic dynamics.

To this end, we shall present an electronic analog study of the crisis effects in a symmetrical two-well potential forced oscillator, which also represents the dynamics of a buckled beam[9] as well as a plasma oscillator.[10] Its dynamics of motion can be modeled by the following equation as

$$\ddot{X}+K\dot{X}+dV(X)/dX=F\sin(\omega t)\ , \tag{1}$$

where K is the damping coefficient, F is the driving force, ω is the driving frequency, and $V(X)$ is the potential. For a two-well case, the potential $V(X)$ is given by

$$V(X)=\tfrac{1}{2}\alpha X^2+\tfrac{1}{4}\beta X^4 \tag{2}$$

with $\alpha<0$ and $\beta>0$. Thus, it has a central potential barrier around $X=0$ and two stable equilibra at $X=\pm(-\alpha/\beta)^{1/2}$ as shown in Fig. 1. And Eq. (1) becomes an ordinary differential equation of Duffing type as

$$\ddot{X}+K\dot{X}+\alpha X+\beta X^3=F\sin(\omega t)\ . \tag{3}$$

The chaotic motions in Eq. (3) have been investigated by many authors in the past few years.[11] It is known that, at a certain situation, the motion swings chaotically between the two valleys as a hopping state. The features of the hopping state such as the fractal dimension of both the strange attractor and basin boundary,[12,13] the $1/f$ low frequency spectrum,[14] and the similarity exponents[15] have been found, respectively. In spite of such considerable efforts so far, properties of the crisis in this system have not yet been pointed out. The goal of this paper, therefore, is to increase our understanding of the crisis event in the Duffing equation. The important roles of the symmetry and nonlinearity of the central barrier of the potential well in the occurrence of crises are also emphasized.

The selection of the analog simulator which is constructed with two usual integrators and two multipliers is based on the following reasons. It has the advantage of fast response over the numerical calculations as the parameters are varied, so that it enables us to uncover quickly a guideline by which a more precise study of the nu-

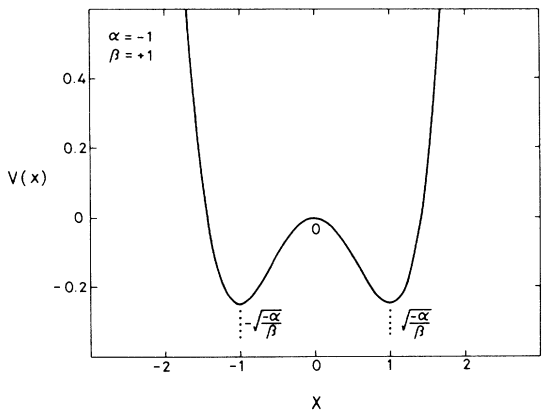

FIG. 1. Symmetrical two-well potential $V(X)$ with a central barrier at $X=0$.

merical calculation can be followed. Moreover, together with a sample-hold circuit, it shows directly a return map of the attractor on the scope so that the detailed features of the crisis can be effectively traced.

II. EXPERIMENTAL RESULTS

As pointed out in our previous paper,[5] the dynamic behaviors in Eq. (3) can be properly investigated by scanning either the driving amplitude F or frequence ω with coefficients K, α, and β as parameters. From variations of the phase portrait $\dot{X}$ versus X and/or the return map a state diagram which illustrates the thresholds of hysteresis jump, period doubling, and crisis in F versus ω space is constructed. The return map characterizes the voltage of variable X at any instant, X_{n+1}, as a function of the same voltage but one period earlier, X_n. A typical case with $K=0.1$, $\alpha=-1$, $\beta=1$, and $0.5<\omega<1.4$ is shown in Fig. 2. In this figure there are two similar groups of threshold curves related to the primary and secondary resonances with ω in the ranges 0.8—1.4 and 0.5—0.7, respectively. Both behave in a global manner.[16] For convenience, we focus only on the former case. Curves A and A' are the downward-jump threshold, curves B and B' are the upward-jump threshold, curve C is the period-doubling threshold, and curve D is the threshold of boundary crisis. These curves intersect each other at critical points (F_{AB},ω_{AB}) for curves A and B, (F_{AD},ω_{AD}) for curves A and D, and (F_{BD},ω_{BD}) for curves B and D, respectively. With reference to Fig. 2, there are two types of both crisis and hysteresis, respectively, depending on the scanning procedures. The salient features of each scanning are summarized below.

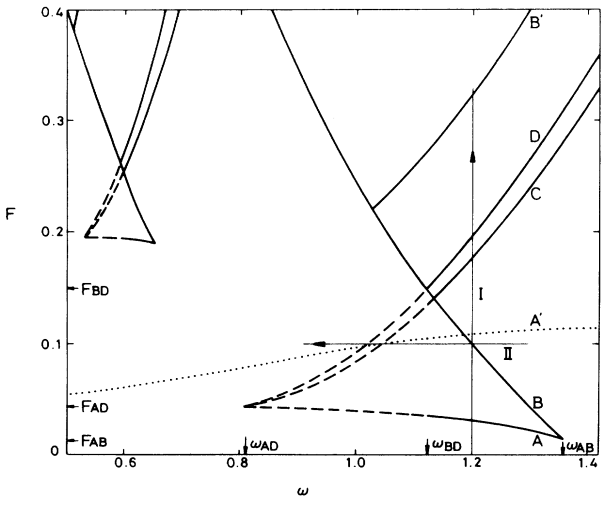

FIG. 2. State diagram in the parameter space F vs ω with threshold curves; A, A': downward jump; B, B': upward jump; C: period doubling; D: boundary crisis, with damping coefficient $K=0.1$. All dashed curves are obtained with an initial state above curve B. The dotted curve A' is obtained with an initial state above curves B' and B.

A. Amplitude scanning

1. $\omega>\omega_{BD}$

For a typical demonstration of the results, we choose $\omega=1.2$, a value larger than ω_{BD} $(=1.125)$, and set initially the state at the equilibrium point $X=1.0$. As the driving amplitude F is increased from zero (path I), a sequence of transitions occur on the threshold curves. The phase portraits near these transitions are shown in Fig. 3. First of all, on curve B with $F=0.097$, the unsymmetrical phase portrait expands abruptly as shown in Fig. 3(a). This behavior is referred as upward jump. On the contrary, while F is turned back from above curve B, the phase portrait is restored suddenly to the initial shape on curve A with $F=0.033$. This is referred to as a downward jump. Hence, curves A and B form a hysteresis loop with the motion confined only in the right valley. Note that, in these situations, the nonlinear effect is small.

As F is increased to 0.182 on curve C, the threshold of period doubling, the phase portrait splits into two cycles as shown in Fig. 3(b). The state undergoes the Feigenbaum's route to chaos soon after period four as F is further increased. It implies that the nonlinear effect is strong enough to cause the chaotic motion. Due to a less steep slope of the potential well around the central barrier, the trajectory of the phase portrait in the left-hand side splits much more distinctly and approaches to the unstable equilibrium point at $X=0$. In other words, the separation of the trajectory is essentially dependent on the slope of the potential well. When F is increased a little bit to 0.198 on curve D, the onset of crisis, the motion begins to migrate into the left valley and exhibits a hopping state as shown in Fig. 3(c). We refer to it later as crisis-induced hopping.

As F is further increased, the state keeps on hopping first and then is locked to some subharmonics. Figure 3(d) shows the phase portrait of a typical case for $\frac{1}{5}$ subharmonic with $F=0.268$. This state exists in a small interval of the driving amplitude. As F is increased to 0.321 on curve B', the hopping state disappears suddenly and becomes stable with a symmetrical phase portrait extending over the two valleys as shown in Fig. 3(e). It implies that the central barrier plays no significant effect on the motion for large excitations. In other words, the system is again in a situation with small nonlinearity.

Alternatively, if the amplitude F is decreased from above curve B', a downward jump occurs at $F=0.110$ on curve A'. The larger symmetrical phase portrait is restored abruptly to a smaller nonsymmetrical one as shown in Fig. 3(f). Note that curve A' is found only when the initial state is above both curves B and B'. This unusual type of hysteresis with a great contraction implies a catastrophe associated with a symmetry breaking and ought to receive more attention.

Now, in order to elucidate the features of crisis occurring on curve D, the corresponding return maps as shown in Fig. 4 are traced. Figure 4(a) shows the return map of the chaotic attractor between the cascaded period doublings and crisis with $F=0.194$. The map is similar to a quadratic form, however, with a back-folded tail (mark).

As F is further increased, the folded tail extends more and more close to the line with $X_{n+1}=X_n$. At $F=0.198$ on curve D the tail meets at a point (mark) on the line $X_{n+1}=X_n$. The point is referred to as an unstable fixed point with a slope dX_{n+1}/dX_n larger than 1 as shown in Fig. 4(b). This case implies the occurrence of a boundary crisis.[3] In this moment, the motion in the right valley at $X>0$ jumps into the left one at $X<0$ and, meanwhile, develops a new part of the chaotic attractor with the similar quadratic shape. Therefore, it is a nondestructive type of boundary crisis with abrupt expansion of the strange attractor.

Similarly, the dynamic process of the state in the left valley moving to the right one behaves in the same manner as just mentioned. Thus, a crisis-induced hopping between the two strange attractors appears. This feature

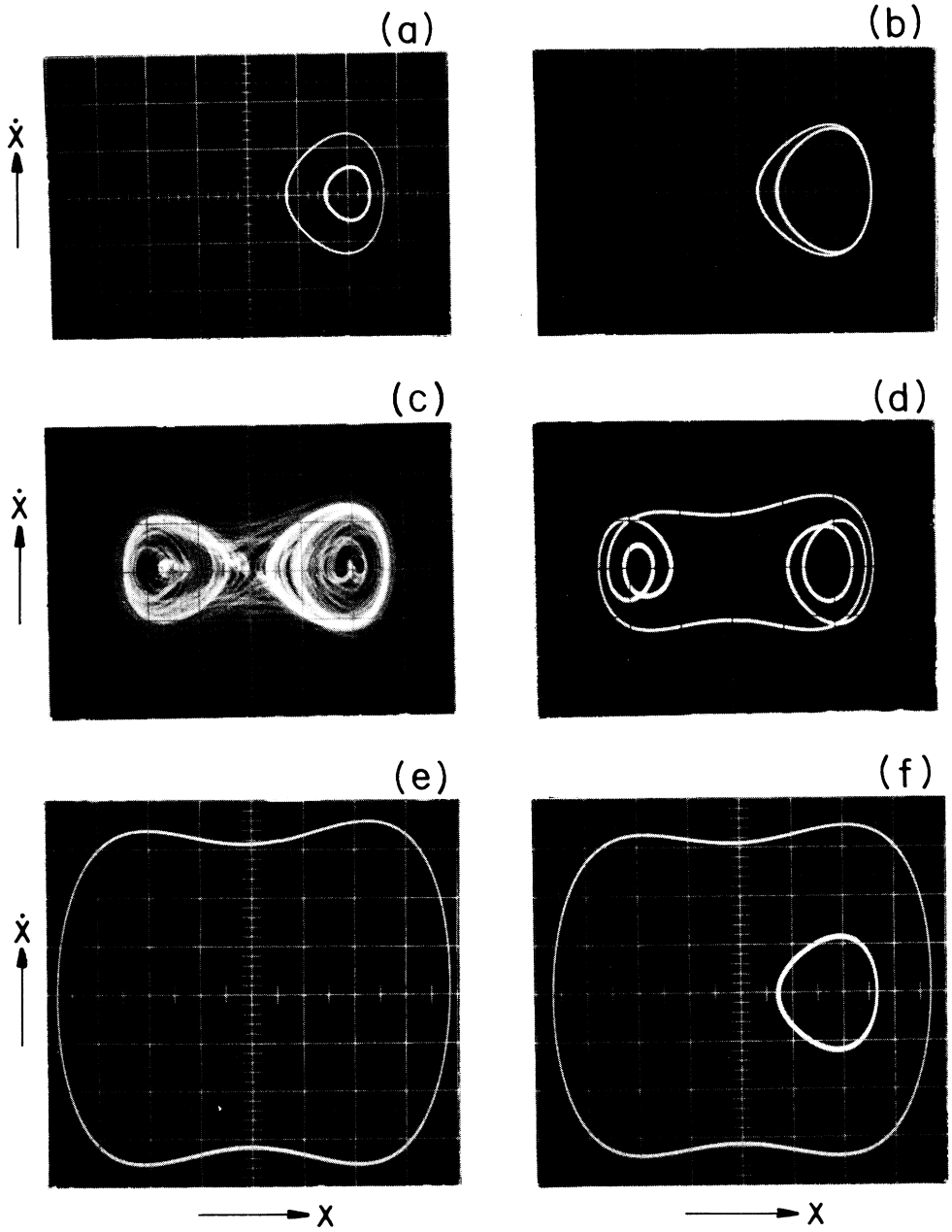

FIG. 3. Phase portraits for $\omega=1.2$ and (a) $F=0.092$, the states just below (small) and above (large) curve B; (b) $F=0.182$, the period-doubled state just above curve C; (c) $F=0.198$ the hopping state just above curve D; (d) $F=0.268$, the $\frac{1}{5}$ subharmonic state; (e) $F=0.321$, the state just above curve B'; (f) $F=0.110$, the state just above (large) below (small) curve A'. X axis: X, $0.5v$/div. Y axis: X, $0.5v$/div.

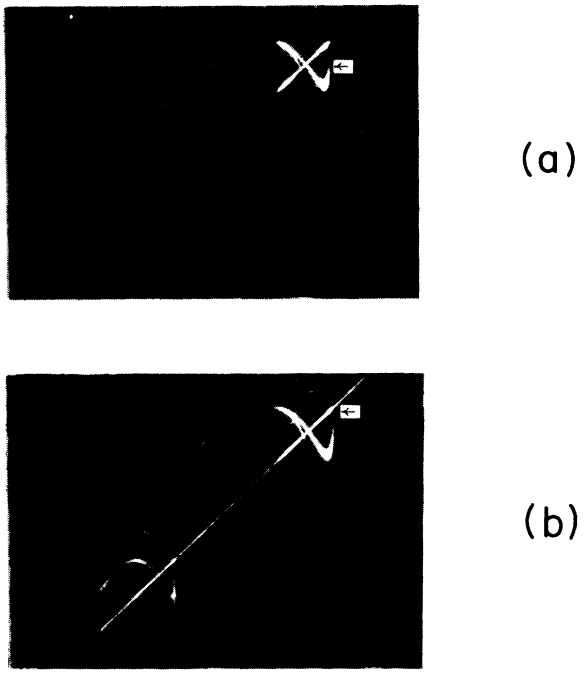

FIG. 4. Return maps with $\omega=1.2$ and (a) $F=0.194$, before crisis; (b) $F=0.198$, crisis occurring on curve D.

is due to the nature of the symmetrical property of the potential well. According to our observations, the state is about equally likely to be in each valley of the potential well and give rise to the low-frequency noise with approximate $1/f$ shape as shown in Fig. 5.

2. $\omega<\omega_{BD}$

In this range, curves A, C, and D (dashed part) are not found from this scanning process, because the process is reversible. The hopping state above curve B directly returns back to the initial stable state once the amplitude F is lowered just below curve B and vice versa.

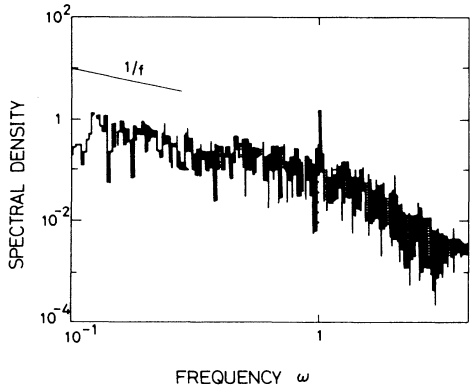

FIG. 5. Spectrum of the voltage signal $X(t)$ for crisis-induced hopping with $F=0.199$ and $\omega=1.2$.

B. Frequency scanning

To find the dashed part of curves A, C, and D we investigate alternatively the dynamic process by frequency scanning.

1. $F>F_{AD}$

In the present case we choose $F=0.100$, a value between the critical ones of F_{BD} $(=0.150)$ and F_{AD} $(=0.045)$ as indicated in Fig. 2. As the frequency ω is lower down from 1.3 (path II) with the initial state above curve B, the Feigenbaum route to chaos is first seen with onset of period two at $\omega=1.048$ on curve C and then the boundary crisis occurs at $\omega=1.023$ on curve D. The return map is shown in Fig. 6(a) where the strange attractor contracts suddenly to a fixed point either in the original right valley or in the left one rather than hopping. In such a case the boundary crisis is referred to as destructive. Figure 6(b) shows the sampled signal X_n as a function of frequency. It demonstrates the destructive feature

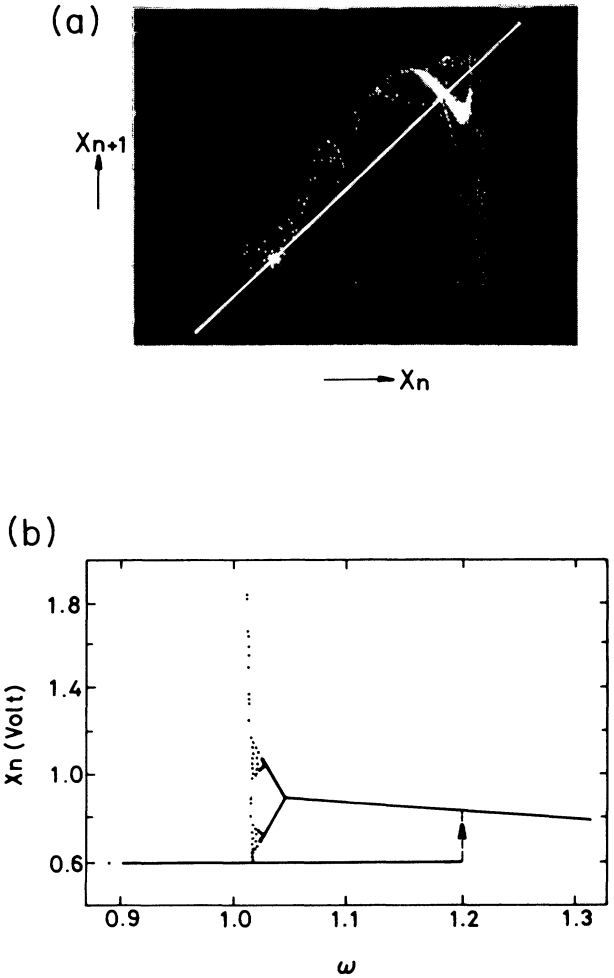

FIG. 6. (a) Return map of boundary crisis with $F=0.100$ and $\omega=1.023$, (b) response of voltage X_n as a function of ω with $F=0.100$.

with hysteresis after a cascade of period doublings. When F is set larger than F_{BD}, the crisis with hopping occurs on curve D. The map is similar to Fig. 4(b). Hence curve B plays an important role in differentiating these two distinct types of boundary crisis.

2. $F < F_{AD}$

However, if the driving amplitude F is chosen between $F_{AD} > F > F_{AB}$ (0.015), then a hysteresis jump is observed without any bifurcation or crisis occurring. Also, as F is less than F_{AB}, the hysteresis disappears.

III. CONCLUSION

In this paper we have presented as intensive study of an analog simulation for nonlinear oscillation with application to the Duffing equation. Owing to the nonlinear effect, the dissipative system exhibits the following transition sequences: hysteresis, period doublings, and crises with a global manner. The thresholds are shown in a state diagram from which the transitions can be easily referred to.

Two types of hysteresis are observed. One is accompanied by a symmetry breaking of the phase portrait as occurred from a symmetrical two-valley to asymmetrical one-valley motion. The other is confined to a one-valley motion only. The former case with the symmetry breaking appears to be a large size contraction of the phase portrait.

Two types of boundary crisis are also observed. One is associated with a hopping between two strange attractors, and the other is associated with a destruction of the chaotic attractor accompanying a hysteresis jump. The former is also confirmed to have $1/f$ low-frequency noise. The hysteresis upward-jump curve B acts as the borderline for these two distinct types of crisis.

Our study not only supports the conjecture of Grebogi *et al.*, but also further presents the persistent properties of the crisis related to the symmetrical property and the height of the central potential barrier in the Duffing equation.

[1]E. Ott, Rev. Mod. Phys. **53**, 655 (1981).
[2]J. P. Eckmann, Rev. Mod. Phys. **53**, 643 (1981).
[3]C. Grebogi, E. Ott, and J. A. Yorke, Phys. Rev. Lett. **48**, 1507 (1982); Physica **7D**, 181 (1983).
[4]E. G. Gwinn and R. M. Westervelt, Phys. Rev. Lett. **54**, 1613 (1985); H. Chat'e and P. Manneville, Phys. Rev. A **32**, 3065 (1985).
[5]Y. H. Kao, J. C. Huang, and Y. S. Gou, Phys. Rev. A **34**, 1682 (1986).
[6]B. A. Huberman and J. P. Crutchfield, Phys. Rev. Lett. **23**, 1743 (1979).
[7]R. W. Rollins and E. R. Hunt, Phys. Rev. A **29**, 3327 (1984); H. Ikezi, J. S. deGrassie, and T. H. Jensen, Phys. Rev. A **28**, 1207 (1983); C. Jeffries and J. Perez, Phys. Rev. A **27**, 601 (1983).
[8]F. T. Arecchi, R. Badii, and A. Politi, Phys. Lett. **103A**, 3 (1984).
[9]F. C. Moon and P. J. Holmes, J. Sound Vib. **65**, 275 (1979).
[10]R. A. Mahaffey, Phys. Fluids **19**, 1387 (1976).
[11]J. Guckenheimer and P. Holmes, *Nonlinear Oscillators, Dynamical Systems, and Bifurcations of Vector Field* (Springer, New York, 1983).
[12]F. C. Moon and G.-X. Li, Physica **17D**, 99 (1985).
[13]F. C. Moon, Phys. Rev. Lett. **53**, 962 (1984).
[14]F. T. Arecchi and F.Lisi, Phys. Rev. Lett. **49**, 94 (1982); F. T. Arecchi and A. Califano, Phys. Lett. **10A**, 443 (1984).
[15]H. Ishii, H. Fujisaka, and M. Inoue, Phys. Lett. **116A**, 257 (1986).
[16]U. Parlitz and W. Lauterborn, Phys. Lett. **107A**, 351 (1985); S. Sato, M. Sano, and Y. Sawada, Phys. Rev. A **28**, 1654 (1983).

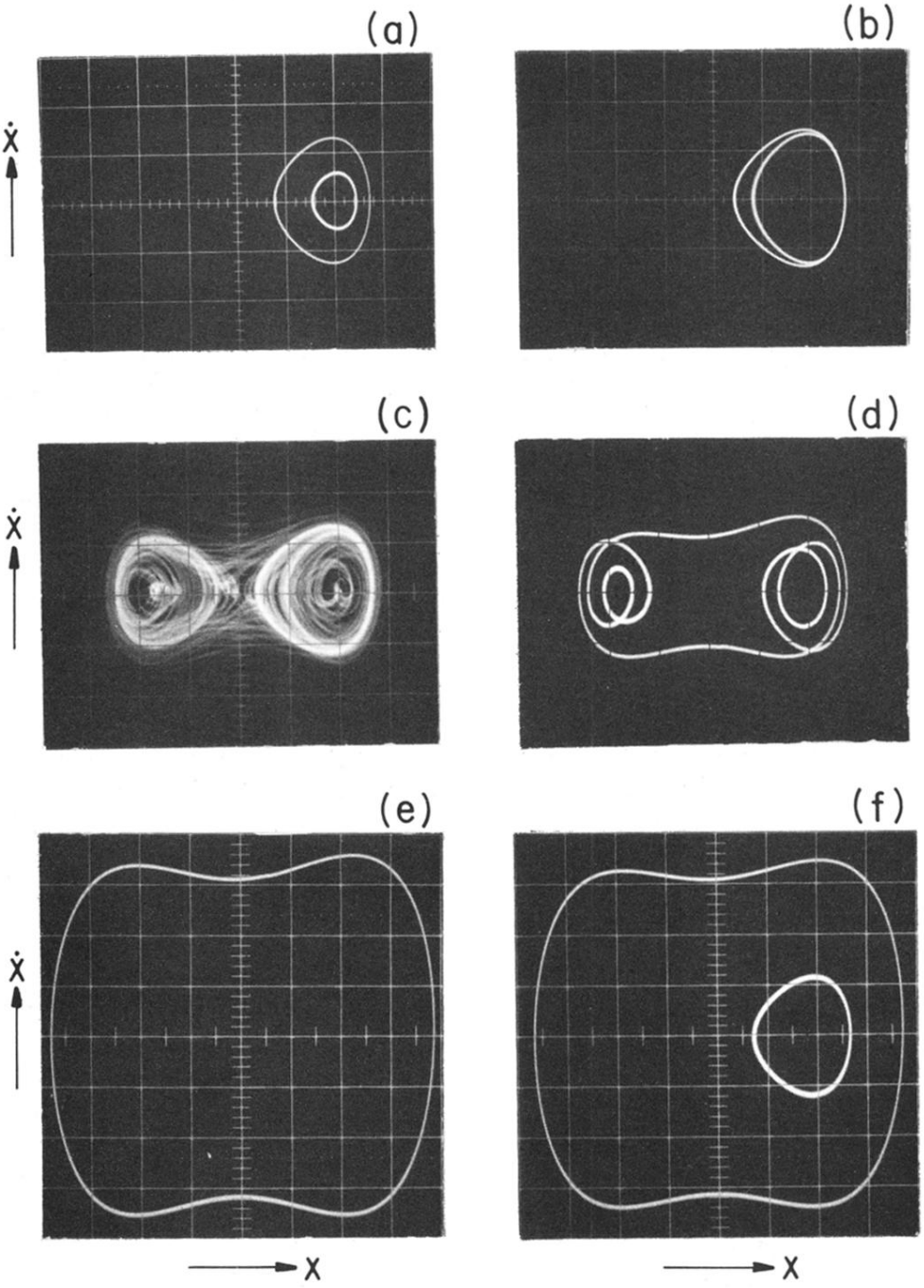

FIG. 3. Phase portraits for $\omega=1.2$ and (a) $F=0.092$, the states just below (small) and above (large) curve B; (b) $F=0.182$, the period-doubled state just above curve C; (c) $F=0.198$ the hopping state just above curve D; (d) $F=0.268$, the $\frac{1}{5}$ subharmonic state; (e) $F=0.321$, the state just above curve B'; (f) $F=0.110$, the state just above (large) below (small) curve A'. X axis: X, $0.5v$/div. Y axis: X, $0.5v$/div.

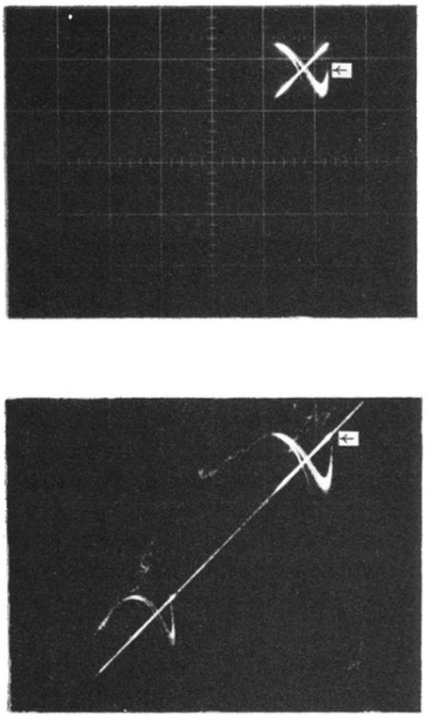

FIG. 4. Return maps with $\omega = 1.2$ and (a) $F = 0.194$, before crisis; (b) $F = 0.198$, crisis occurring on curve D.

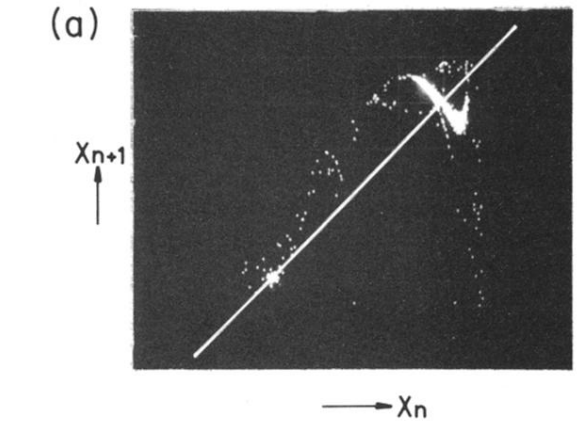

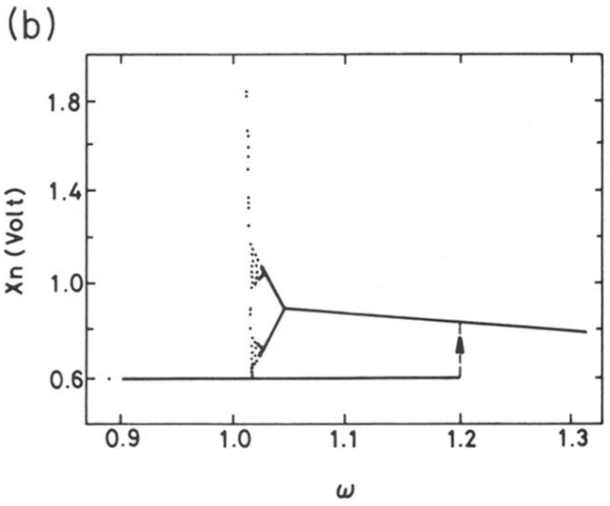

FIG. 6. (a) Return map of boundary crisis with $F=0.100$ and $\omega=1.023$, (b) response of voltage X_n as a function of ω with $F=0.100$.